Detection of race-specific resistance against *Puccinia coronata* f. sp. *avenae* in *Brachypodium* species

Vahid Omidvar, Sheshanka Dugyala, Feng Li, Susan Rottschaefer, Marisa E. Miller, Mick Ayliffe, Matthew J. Moscou, Shahryar F. Kianian, Melania Figueroa.

First, second, third, fourth, fifth, eighth and ninth authors: Plant Pathology, University of Minnesota, St. Paul, MN, USA; sixth author: CSIRO Agriculture and Food, ACT, Australia; seventh author: The Sainsbury Laboratory, Norwich Research Park, Norwich NR4 7UH, UK; eighth author: Cereal Disease Laboratory, United States Department of Agriculture-Agricultural Research Service, St. Paul, MN, USA; ninth author: Stakman-Borlaug Center for Sustainable Plant Health, University of Minnesota, St. Paul, MN, USA.

Correspondence: Melania Figueroa; email: figue031@umn.edu; Tel: +1 612 624 2291

Abstract

Oat crown rust caused by *Puccinia coronata* f. sp*. avenae* is the most destructive foliar disease of cultivated oat. Characterization of genetic factors controlling resistance responses to *Puccinia coronata* f. sp*. avenae* in non-host species could provide new resources for developing disease protection strategies in oat. We examined symptom development and fungal colonization levels of a collection of *Brachypodium distachyon* and *B. hybridum* accessions infected with three North American *P. coronata* f. sp*. avenae* isolates. Our results demonstrated that resistance phenotypes are dependent on both host and pathogen genotypes, indicating a role for race-specific responses in these interactions. These responses were independent of the accumulation of reactive oxygen species. Expression analysis of several defense-related genes suggested that salicylic acid and ethylene-mediated signaling, but not jasmonic acid are components of resistance reaction to *P. coronata* f. sp*. avenae*. Our findings suggest that effector-triggered immunity contributes to non-host resistance to *P. coronata* f. sp*. avenae* in *Brachypodium* species and provide the basis to conduct a genetic inheritance study to examine this hypothesis.

Keywords non-host, oat, crown rust, resistance, susceptibility, effector

Introduction

Oat crown rust caused by the obligate biotrophic rust fungus *Puccinia coronata* f. sp. *avenae* is the most widespread and damaging foliar disease of cultivated oat (*Avena sativa* L.) (Nazareno et al. 2017). Symptoms of crown rust infection manifest in the foliar tissue, causing a reduction in photosynthetic capacity and thus affecting grain size and quality (Holland and Munkvold 2001; Simons 1985). The most sustainable method to control this devastating disease is the use of genetic resistance (Carson 2011). Novel sources of genetic resistance may therefore translate into novel crop protection strategies.

In general, plant disease resistance to would-be pathogens can be conferred by either constitutive or induced barriers (Heath 2000; Nurnberger and Lipka 2005). Physical barriers, such as rigid cell walls and waxy cuticles as well as preformed antimicrobial compounds are some of the constitutive obstacles that explain why plants are immune to most microbes. Nevertheless, certain microbes have evolved strategies to overcome these barriers, and in such instances plant-microbe incompatibility is based upon pathogen recognition and the induction of plant defense responses (Heath 2000, Periyannan et al. 2017).

Inducible defense responses in plants are mediated by a tightly regulated two-tier immune recognition system that, depending on the physiological characteristics of the potential pathogen, may or may not be effective at preventing microbial colonization (Dodds and

Rathjen 2010). The first layer of microbial recognition is controlled by cell surface associated receptors, named pattern recognition receptors (PRRs). PRRs recognize conserved and essential microbial molecules known as pathogen-associated molecular patterns (PAMPs) and/or plant derived damage-associated molecular patterns (DAMPs). This recognition leads to the activation of a range of broad-spectrum basal defenses that constitute PAMP-triggered immunity (PTI) (Zipfel 2008). PAMPs in pathogenic fungi like the crown rust pathogen include chitin or xylanases, which are essential constituents of the fungal cell wall. In contrast, DAMPs are not necessarily pathogen derived and include plant cell wall fragments and plant peptides released during infection.

Adapted pathogens manipulate PTI signaling events and suppress basal defenses by secreting a suite of effector proteins into plant cells, thereby enabling successful plant colonization in some instances (Toruno et al. 2016). However, disease resistance against adapted pathogens can still occur if the plant can recognize one or more of these secreted effector molecules. Effector recognition generally occurs by plant intracellular nucleotide binding leucine rich repeat (NB-LRR) receptors that each induce defense responses upon recognition of a cognate pathogen effector, also known as an avirulence (Avr) protein. This second layer of pathogen recognition, referred to as effector-triggered immunity (ETI), frequently results in a localized hypersensitive cell death response at attempted infection sites (HR) and is the underlying molecular basis of the gene-for-gene concept (Dodds and Rathjen 2010; Ellis et al. 2014; Flor 1971). ETI is highly specific with resistance only occurring if the adapted pathogen isolate expresses an effector that is recognized by a corresponding NB-LRR in the infected plant.

The delivery of rust effector proteins into host plants is mediated by distinct fungal infection structures called haustoria (Catanzariti et al. 2006; Garnica et al. 2014; Panstruga and Dodds 2009). Only a small number of effectors have been characterized in rust fungi (Chen et al. 2017; Maia et al. 2017; Ravensdale et al. 2011; Salcedo et al. 2017), however, genome-wide effector mining suggests that rust pathogens may deploy hundreds of effector molecules via the haustorium during infection (Cantu et al. 2013; Duplessis et al. 2011; Hacquard et al. 2012; Nemri et al. 2014; Rutter et al. 2017). Oat crown rust populations are typified by a complex race-structure, which likely originates from variation in the array of effectors present in different pathogen genotypes (Carson 2011; Chong et al. 2000; Nazareno et al. 2017). For years, oat breeding programs have relied upon naturally occurring resistance in *Avena* spp., most likely mediated by *NB-LRR* genes, to protect against crown rust. However, the resistance of these oat varieties is often rapidly overcome by evolution of the crown rust pathogen to avoid host plant recognition. Achieving increased durability in oat crown rust resistance therefore requires new sources of genetic immunity to be identified and further advances made in our understanding of the molecular basis of rust recognition in host and non-host plant species.

Non-host plant species potentially offer an untapped resistance resource. Non-host resistance (NHR) is typically described in the context of a dichotomy that distinguishes it from host resistance. NHR is defined as genotype-independent and effective against all genetic variants of a non-adapted pathogen species, whereas host resistance is

genotype-dependent and effective only against a subset of genetic variants of an adapted pathogen (Mysore and Ryu 2004). This paradigm has been gradually changing as accumulating evidence suggests that signaling pathways and defense mechanisms overlap in non-host and host resistance and that microbial adaptation to plant species does not conform to a simple qualitative distinction (Bettgenhaeuser et al. 2014; Dawson et al. 2015; Figueroa et al. 2015; Gill et al. 2015; Thordal-Christensen 2003). Instead, disease phenotypes observed for different plant and pathogen interactions span a continuous spectrum of outcomes ranging from immunity to susceptibility, with many intermediate interactions, making the classification of non-host versus host systems problematic (Bettgenhaeuser et al. 2014; Dawson et al. 2015). Regardless of the terminology, identifying the molecular determinants of non-host or intermediate resistance is of great interest as this type of resistance could be durable and broad-spectrum and contribute significantly to crop improvement.

Brachypodium distachyon, a small grass closely related to cereals, is considered a non-host to several rust fungi species related to *P. coronata* f. sp*. avenae*, such as *Puccinia emaculata*, *Puccinia striiformis, Puccinia graminis* and *Puccinia triticina* (Ayliffe et al. 2013; Barbieri et al. 2011; Bettgenhaeuser et al. 2014; Bossolini et al. 2007; Dawson et al. 2015; Figueroa et al. 2013, 2015; Gill et al. 2015). Variation in fungal colonization in some of these interactions suggests that it may be possible to genetically dissect these types of immune responses and harness them for engineering rust disease resistance (Figueroa et al. 2015). In this study, we examined the interaction between *P. coronata* f. sp*. avenae* and *B. distachyon*, as well as *Brachypodium hybridum*. *B. hybridum* is an

143 allotetraploid species originated from the hybridization of the diploid species *B. distachyon*
144 *and B. stacei* (Lopez-Alvarez et al. 2012).
145
146 Pathogen susceptibility in plants, particularly to rust fungi, is a process, which remains
147 poorly characterized. Our study shows that *P. coronata* f. sp*. avenae* can infect *B.*
148 *distachyon* and *B. hybridum* leaves and grow extensively, but cannot sporulate. These
149 findings open the possibility of investigating mechanisms that confer partial rust
150 susceptibility in *Brachypodium.* Gene expression analysis of an ortholog of the putative
151 rust susceptibility factor in wheat, which encodes a hexose transporter (Moore et al.
152 2015), suggested that sugar transport may also be important to sustain the growth of *P.*
153 *coronata* f. sp*. avenae* in *B. distachyon.* In addition to this, we found evidence for race-
154 specific resistance in both species supporting the model proposed by Schulze-Lefert and
155 Panstruga (2011), which postulates a role of ETI in NHR due to the phylogenetic
156 relatedness between the non-host and host species. These findings provide a framework
157 to conduct genetic inheritance studies to dissect recognition of *P. coronata* f. sp. *avenae*
158 by *B. distachyon* and *B. hybridum* and identify loci governing intermediate oat crown rust
159 susceptibility.
160
161 **Materials and Methods**
162
163 **Plant and fungal materials**
164
165 Twenty-two accessions of *B. distachyon* (ABR6, ABR7, Adi12, Adi13, Adi15, Bd1-1,

Bd18-1, Bd21, Bd21-3, Bd2-3, Bd29-1, Bd30-1, Bd3-1, BdTR10H, BdTR13K, Foz1, J6.2, Jer1, Koz5, Luc1, Mon3, and Tek4) and three accessions of *B. hybridum* (Bou1, Bel1, and Pob1) were used in this study. Seeds were obtained from the John Innes Centre (Dawson et al. 2015), Aberystwyth University (Mur et al. 2011), Joint Genome Institute and Montana State University (Vogel et al. 2009), Universidad Politécnica de Madrid (Dr. Elena Benavente) and USDA-ARS Plant Science Unit, St. Paul, MN, U.S.A (Garvin et al. 2008). All plants were increased by single seed descent prior to conducting this study. The cultivated oat (*Avena sativa*) variety Marvelous was used as a susceptible host to *P. coronata* f. sp*. avenae*. This study used three North American oat crown rust isolates, 12NC29 (race LBBB) and 12SD80 (race STTG) (Miller et al. 2018) collected in 2012, and a historic race 203 (race QBQT) known to be avirulent to the oat variety Victoria (Chang and Sadanaga 1964). Isolates were obtained from the rust collection available at the USDA-ARS Cereal Disease Laboratory, St. Paul, MN, U.S.A.

Inoculation and pathogen assays

Brachypodium and oat seedlings were grown with 18/6 h light/dark, 24/18°C day/night cycles and 50% humidity. Urediniospores were activated by heat shock treatment at 45ºC for 15 min to break cold induced dormancy and suspended in an oil carrier (Isopar M, ExxonMobil) for spray inoculation. Seedlings of *Brachypodium* accessions and oat were inoculated using 50 µL of each *P. coronata* f. sp*. avenae* inoculum (10 mg urediniospores/mL) at three-leaf and first-leaf stages, respectively. For mock inoculation, seedlings were sprayed with oil without urediniospores. Infected seedlings were placed

in dew chambers in the dark for 12 h with intermittent misting for 2 min every 30 min. After 12 h, misting was stopped and seedlings were exposed to light for 2 h before they were placed back in growth chambers. Infected primary leaves of oat and secondary leaves of *Brachypodium* accessions were collected for analysis. Macroscopic symptoms were evaluated at 14 days post infection (dpi). Digital images were captured using a stereomicroscope (Olympus model SZX16).

Analysis of fungal colonization by microscopy

Both infected secondary *Brachypodium* leaves at 14 dpi and infected primary *A. sativa* (variety Marvelous) leaves at 12 dpi were cut into 1 cm length sections and stained with wheat germ agglutinin Alexa Fluor® 488 conjugate (WGA-FITC; ThermoFisher Scientific) to visualize fungal colonies as previously described (Ayliffe et al. 2013; Dawson et al. 2015). Visualization of fungal intracellular growth was carried out using a fluorescence microscope (Leica model DMLB) under blue light with a 450-490 nM excitation filter. The percentage of leaf colonized (pCOL) by *P. coronata* f. sp. *avenae* was estimated according to the method of Dawson et al. (2015) with a modification to report 0, 0.5, 0.75, and 1 scores for disjointed fields of view with hyphal growth less than 15%, between 15-50%, 50-75%, and greater than 75%, respectively. Two independent biological replicates were evaluated per *P. coronata* f. sp. *avenae* isolate (12SD80, 203, and 12NC29) and each biological replicate included three leaves. pCOL values from all three leaves were combined to obtain a mean and standard error of the mean. Fungal development was also examined in whole-mounted infected leaves of *B. distachyon* accessions ABR6 and

Bd21 and oat at 1, 2, 3, and 6 dpi. The percentage of urediniospores that successfully germinated and formation of various infection structures, including appresorium (AP), substomatal vesicle (SV), haustorium-mother cell (HMC), and established colonies (EC), were recorded in WGA-FITC stained samples. Three independent biological replicates were evaluated per *P. coronata* f. sp*. avenae* isolate (12SD80, 203, and 12NC29).

Analysis of H_2O_2 accumulation

H_2O_2 accumulation was evaluated using 3,3′-diaminobenzidine (DAB) staining as described by Thordal-Christensen et al. (1997). Infected leaves were stained in 1 mg/mL DAB aqueous solution at pH 3.8 for 4 h in dark and destained in Farmer's fixative for 12 h. The number of infection sites displaying H_2O_2 accumulation per biological replicate per isolate was recorded using a light microscope (Leica model DMLB). Each biological replicate included one to two infected secondary leaves to account for 100 infection sites. Data represents the sum of all infection sites displaying H_2O_2 accumulation in three biological replicates.

Quantification of fungal biomass by DNA quantification

Genomic DNA was extracted from infected and mock-treated secondary leaves of *B. distachyon* accessions ABR6 and Bd21 at 3, 7, and 12 dpi using DNeasy Plant Mini Kit (Qiagen). The relative abundance of fungal DNA was measured using the Femto™ Fungal DNA Quantification Kit (Zymo Research) based on quantification of ITS regions using ITS-specific primers and fungal DNA Standards provided by the manufacturer. PCR

was conducted using a CFX96 Real-Time system (Bio-Rad) and thermal cycles were set for initial denaturation at 95°C for 10 min, 45 cycles of 95°C for 30 s, 50°C for 30 s, 60°C for 60 s, followed by a final extension cycle at 72°C for 7 min. The *Brachypodium GAPDH* gene was also quantified in the same DNA samples using gene-specific primers (Hong et al. 2008). Fungal DNA level was normalized relative to the plant *GAPDH* value in each sample. At least four biological replicates were analyzed per time point per isolate, with two technical replicates within each biological replicate.

RNA extraction and RT-qPCR analysis

Total RNA was extracted from infected and mock-treated secondary leaves of *B. distachyon* accessions ABR6 and Bd21 at 12, 24, 48, and 72 hpi using the RNeasy Plant Mini Kit (Qiagen). For RT-qPCR, cDNA was synthesized using the PrimeScript First Strand cDNA Synthesis Kit (Takara) and amplification was performed using the SensiFAST SYBR Lo-ROX Kit (Bioline). Sequences of gene-specific primers, reported by Gill et al. (2015) and Mandadi and Scholthof (2012) and those used in our study are listed in Supplementary Table 1. Expression levels were normalized using the plant *GAPDH* gene (Hong et al. 2008). PCR thermal cycles were set for initial denaturation at 95°C for 2 min, 40 cycles of 95°C for 5 s, followed by annealing/extension at 60°C for 20 s in a CFX96 Real-Time PCR system (Bio-Rad). Data was collected from three biological replicates with two technical replicates within each. Differential expression (DE) values were calculated as normalized fold changes of the expression using the ΔΔCT method (Livak and Schmittgen 2001), and DE value ≥ 2 was considered as a significant change

in gene expression.

Results

Variation in resistance response of *Brachypodium* accessions to *P. coronata* f. sp. *avenae* infection

To examine the ability of *P. coronata* f. sp. *avenae* to infect non-host species *B. distachyon* and *B. hybridum* we evaluated the disease responses of 25 different *Brachypodium* accessions to three North American *P. coronata* f. sp. *avenae* isolates, 12SD80, 203, and 12NC29 (Fig. 1A). All three isolates are fully virulent on the susceptible oat variety Marvelous with obvious sporulation occurring (Fig 1B, C). In contrast, no pustules were observed on any *Brachypodium* accession 30 days post-infection, which suggests that the asexual phase of the *P. coronata* f. sp. *avenae* life cycle cannot be completed on either *B. distachyon* or *B. hybridum.* However, macroscopic symptoms were observed on *Brachypodium* accessions in response to challenge with these rust isolates (Fig. 1D, E, Table 1) with some accessions developing chlorosis and/or necrosis of varying severity (Fig. 1F, Table 1). These symptoms were dependent upon both the accession genotype and rust genotype. For example, the necrosis severity of accession Bd1-1 was high in response to isolate 12SD80 but low upon infection with isolates 203 and 12NC29, whereas chlorosis severity in accession Adi13 was higher when challenged with isolates 12SD80 and 12NC29 but lower in response to isolate 203. Some *Brachypodium* accessions, such as Bd2-3, Bd3-1 and Tek4, reacted differently to all three

rust isolates with different necrosis and chlorosis severities observed in each interaction. ABR6 consistently showed minimal symptom development, whereas accessions such as Bd21, Bd21-3 and Koz5 displayed more extreme necrosis and chlorosis responses to all three isolates.

In parallel, all accessions were analyzed microscopically to determine the extent of *P. coronata* f. sp. *avenae* infection for each isolate. For all three isolates, urediniospores germinated to produce appressoria over stomates that penetrated the stomatal apertures of each accession, indicating that *Brachypodium* accessions are recognized as a potential host by *P. coronata* f. sp. *avenae* (data not shown). A large variation in rust growth was observed amongst these *Brachypodium* accessions (Fig. 2A) although growth was always less than that observed on the oat host. Microscopically no *P. coronata* f. sp. *avenae* isolate showed initiation of uredinia on any *Brachypodium* accession confirming the non-host status of *B. distachyon* and *B. hybridum* to this phytopathogen.

In general, *P. coronata* f. sp. *avenae* isolates 12SD80 and 203, which are more broadly virulent on the oat differentials than isolate 12NC29, showed more extensive growth on all tested *Brachypodium* accessions (Fig. 2A). Isolate 12SD80 showed the most growth, infecting ~79% of the leaf area of accession Bd21-3, while isolate 203 infected ~64% of the leaf area of accession Adi15. In contrast, the maximum growth observed for isolate 12NC29 was ~41% of the leaf area of accession Koz5. For all three isolates, Koz5 and Bd21-3 were amongst those *B. distachyon* accessions with the greatest fungal growth, whereas *B. distachyon* accessions ABR6 and Foz1, as well as *B. hybridum* accession

304 Pob1, had the least fungal growth.

305

306 The fungal growth of each isolate and accession combination was scored relative to the
307 most fungal growth observed for each isolate (Supplementary Fig. 1). Interestingly, some
308 accessions were substantially infected by isolates 12SD80 and 203 while growth of
309 12NC29 was more restricted. For example, accession Bd30-1 had considerable fungal
310 growth of isolates 12SD80 and 203, but only intermediate growth of isolate 12NC29.
311 Similarly, isolates 12SD80 and 203 grew extensively on accession Bd3-1 but growth of
312 isolate 12NC29 was highly restricted. A similar pattern was also observed for accession
313 BdTR10H. In contrast, accession Tek4 was similarly infected by isolates 12SD80 and
314 12NC29, but had greater growth of 203, while isolate 12SD80 grew more prolifically on
315 accession Mon3 than did either isolates 203 and 12NC29.

316

317 Remarkably, symptom development and levels of fungal colonization did not correlate
318 (Table 1, Fig. 2A). For example, Bd29-1 showed extensive necrosis and chlorosis when
319 inoculated with isolate 12SD80 in contrast to 203, but had high levels of colonization by
320 both isolates. Accession Bd18-1 developed the highest necrosis and chlorosis in
321 response to 12NC29 but supported the lowest growth of this isolate. In contrast, the most
322 obvious symptoms on Jer1 correlated with the greatest fungal growth, in this case by
323 isolate 12SD80.

324

325 The variation in fungal growth occurring on different *Brachypodium* accessions suggests
326 that it may be possible to dissect the genetic architecture controlling this NHR against *P.*

coronata f. sp*. avenae*. Given the availability of an ABR6 x Bd21 $F_{4:5}$ *B. distachyon* family (Bettgenhaeuser et al. 2017) and the differences observed in *P. coronata* f. sp. *avenae* infection patterns (Fig. 2A), these two accessions were further analyzed. To further confirm the colonization values estimated for ABR6 and Bd21, fungal biomass accumulation was quantified by qPCR for each rust isolate over a time course experiment of 3, 7 and 12 dpi (Fig. 2B). Biomass of each isolate increased in both accessions; however, significant differences in fungal growth were observed between accessions at 7 and 12 dpi, with qPCR data and fungal colonization estimates clearly correlated. Fungal DNA abundance was higher in accession Bd21 for all three isolates compared with ABR6, while isolate 12NC29 had the least growth on both accessions.

Development of infection structures of *P. coronata* f. sp*. avenae* isolates on *B. distachyon* ABR6 and Bd21

The development of infection structures (Fig. 3A) of isolates 12SD80, 203, and 12NC29 in a 1, 2, 3, and 6 dpi time course experiment was compared between ABR6 and Bd21, with the susceptible oat variety Marvelous included as a positive control. Spore germination rates (GS) and appressorium development (AP) of all three rust isolates were similar on ABR6, Bd21 and oat (Fig. 3B). However, fungal growth on both *Brachypodium* accessions was significantly slower than on susceptible oat, with fewer substomatal vesicles (SV), haustorium-mother cells (HMC) and established colonies (EC) produced at 1, 2 and 3 dpi. The infection progression was generally slower on accession ABR6 than Bd21, while isolate 12SD80 grew at a faster rate on *B. distachyon* compared with the

other two isolates, as demonstrated by the increased percentage of infection sites that formed SV in both accessions at 1 dpi.

Histological analysis of reactive oxygen species in *B. distachyon* ABR6 and Bd21

The production of H_2O_2 was examined in accessions ABR6 and Bd21 upon infection with isolates 12SD80, 203, and 12NC29. Tissues were stained with 3,3′-diaminobenzidine at 1, 2, 3, 4, and 5 dpi (Table 2). H_2O_2 did not accumulate in these accessions in response to infection with isolates 203 and 12NC29, but it was detected in mesophyll cells of ABR6 and Bd21 upon infection with isolate 12SD80 at 2 and 4 dpi, respectively. Despite this only a minority of infection sites showed H_2O_2 accumulation and often H_2O_2 was also present in uninfected tissue. These data suggest that H_2O_2 accumulation is not a common feature of *B. distachyon* NHR to *P. coronata* f. sp. *avenae.*

Transcript profiling of defense-related genes in *B. distachyon* ABR6 and Bd21

To investigate the role of phytohormone-dependent defense responses in *Brachypodium* upon *P. coronata* f. sp. *avenae* infection, the temporal expression profile of several defense-related genes involved in SA, ET, and JA signaling pathways, as well as genes involved in callose synthesis and the phenylpropanoid pathway, were examined. This analysis was undertaken for ABR6 and Bd21 during the early stages of infection (up to 3 dpi), when there were not significant differences in fungal growth among isolates in both accessions (Fig. 2B). In general, expression of genes involved in the SA and ET signaling

pathways were induced in ABR6 and Bd21 during the first 48 h post-infection; however, expression of JA biosynthesis genes was not altered (Fig. 4, Supplementary Fig. 2). Changes in gene expression were greater in ABR6 than Bd21 upon infection with isolates 12SD80 and 203, but the inverse was observed for isolate 12NC29. These findings suggest differences between ABR6 and Bd21 in the early signaling responses to *P. coronata* f. sp. *avenae* infection.

Among the SA signaling pathway genes, expression of *Aberrant Growth Defects 2* (*AGD2*) peaked at 24 to 48 hpi with isolates 12SD80, 203 and 12NC29. The highest upregulation of *AGD2* was observed in the interaction of 12SD80 and ABR6. Expression of *Alternative Oxidase* (*AOX1A*) was induced in ABR6 as early as 12 hpi with isolates 12SD80 and 203, but it was not affected in response to isolate 12NC29. In contrast, *AOX1A* was upregulated in Bd21 only at 48 hpi in response to isolates 12SD80 and 12NC29. The *Pathogenesis-related* (*PR*) genes *PR1* and *PR5* showed the greatest induction amongst all genes tested in response to all three crown rust isolates. The expression of both genes peaked at 48 hpi except for *PR5* expression after inoculation with 12NC29 which peaked at 24 hpi. Overall, induction of these SA-responsive genes occurred in all interactions, but were remarkably stronger in ABR6 when inoculated with 12SD80 and 203, while Bd21 showed similar responses to all three isolates.

Expression of *Ethylene Response Factor 1* (*ERF1*) was maximal at 24 hpi with all three isolates and, as observed for SA-responsive genes, expression of *ERF1* was particularly high in ABR6 in response to isolates 12SD80 and 203. However, expression of an ET

biosynthesis gene, *Aminocyclopropane-1-carboxylic Acid Oxidase* (*ACO1*), two JA biosynthesis genes, *Lipoxygenase 2* (*LOX2*), and *12-oxophytodienoate Reductase 3* (*OPR3*), *WRKY18* transcription factor, and *callose synthase* did not change in either of the accessions in response to challenge with any of the three isolates (Supplementary Fig. 2). Expression of *Phenylalanine Ammonia-Lyase* (*PAL*) was only slightly induced in ABR6 at 12 hpi with isolate 12SD80. *Cinnamyl Alcohol Dehydrogenase* (*CAD*) reached maximum induction in both accessions at 24 to 48 hpi with isolates 12SD80 and 203. In response to infection with isolate 12NC29, this gene was only upregulated in Bd21 between 24 to 48 hpi.

Transcript profiling of *BdSTP13* in *B. distachyon* ABR6 and Bd21

The expression of the *Brachypodium* ortholog of *Lr67 (STP13)* (Bradi1g69710) (Moore et al. 2015) was examined in accessions ABR6 and Bd21 upon infection with all three rust isolates, as it acts as a putative hexose transporter. *BdSTP13* was induced in both accessions in response to the tested rust isolates (Fig. 5). Gene induction peaked at 24 to 48 hpi, except in the interaction between ABR6 and12NC29, which showed low *BdSTP13* transcript accumulation.

Discussion

The lack of effective *P. coronata* f. sp. *avenae* resistance in oat coupled with rapid evolution of pathogen virulence necessitates a search for new sources of resistance to

419 control oat crown rust disease. To explore the potential of using *Brachypodium* species
420 as a germplasm resource for disease resistance against *P. coronata* f. sp. *avenae*, we
421 have characterized the interaction between three *P. coronata* f. sp. *avenae* isolates and
422 a panel of *Brachypodium* accessions, including *B. distachyo*n and *B. hybridum*. At the
423 macroscopic level, variation in resistance phenotypes was observed, which has been
424 previously reported for other rust interactions with *B. distachyon.* In these studies, *P.*
425 *striiformis*, *P. graminis*, and *P. triticina* infection phenotypes varied from immunity to a
426 range of symptoms that included pustule formation and sporulation (Ayliffe et al. 2013;
427 Figueroa et al. 2013; Garvin 2011). However, similar to *Brachypodium-P. emaculata*
428 (switchgrass rust) interactions (Gill et al. 2015), we did not observe *P. coronata* f. sp.
429 *avenae* sporulation on any *Brachypodium* accession, which supports the status of *B.*
430 *distachyon* and *B. hybridum* as non-hosts for this pathogen. Macroscopic infection
431 symptoms were often associated with chlorosis and/or necrosis; however, it was visually
432 difficult to confirm if these symptoms were a consequence of *P. coronata* f. sp. *avenae*
433 infection. Microscopic analysis showed that *P. coronata* f. sp. *avenae* isolates 12SD80,
434 203, and 12NC29 overcame pre-haustorial resistance defenses and were able to colonize
435 leaves of all *Brachypodium* accessions tested. These results are similar to the interactions
436 observed between *P. graminis* f. sp. *tritici* and *B. distachyon* (Ayliffe et al. 2013).
437
438 To better understand the phenotypic variation existing between *P. coronata* f. sp. *avenae*
439 *and Brachypodium* interactions, we compared the extent of fungal growth on a range of
440 accessions. A wide range of pathogen growth was observed on different *Brachypodium*
441 accessions and was dependent on both plant and fungal genotypes. These findings

suggest the presence of race-specific components to resistance, which is likely governed by variation in effector repertoires of the rust isolates and *R* genes present in the *Brachypodium* accessions. Given the close evolutionary relationship between oat and *Brachypodium* spp., it is possible that the accessions included in our study carry *R* genes that can detect effectors of *P. coronata* f. sp. *avenae.* Isolates 12SD80 and 12NC29 display different virulence profiles on the oat differential set and the recent sequencing of these isolates provides evidence of extensive differences in effector gene complements of 12SD80 and 12NC29 (Miller et al. 2018). Future studies identifying and comparing the effector repertoires of rust species, including those in our study and others that infect *Brachypodium* (i.e., *Puccinia brachypodii*) may help to explain our findings.

Although the precise contribution of ETI to non-host rust resistance in *Brachypodium* remains elusive, our findings are generally consistent with the model proposed by Schulze-Lefert and Panstruga (2011), in which ETI is the major contributor to NHR in plant species that are closely related to the natural host. Heterologous expression of fungal and bacterial effectors in several non-host pathosystems supports that effector recognition by immunoreceptors contributes to resistance (Adlung et al. 2016; Giesbers et al. 2017; Lee et al. 2014; Stassen et al. 2013; Sumit et al. 2012), although in some cases effector recognition can occur in the absence of resistance (Giesbers et al. 2017; Goritschnig et al. 2012). Close examination of *Brachypodium* interactions with *P. coronata* f. sp. *avenae* (this study), *P. graminis* ff. spp. *tritici*, *avena* and *phalaridis*, *P. triticina*, and *P. striiformis* suggests that HR-induced cell death is rare (Ayliffe et al. 2013). However, the lack of HR in these interactions does not necessarily undermine the contribution of

ETI to non-host resistance, as there are instances when *R* gene-mediated ETI (e.g., wheat stem rust resistance gene, *Sr33*) can result in resistance without cell death (Periyannan et al. 2013). Further studies are needed to better understand the extent of ETI and HR contributions in non-host resistance given that molecular and genetic factors in these interactions could be pathosystem-specific.

To investigate the role of ROS in the *B. distachyon* response to *P. coronata* f. sp. *avenae,* accessions ABR6 and Bd21, which display contrasting infection phenotypes, were compared. H_2O_2 accumulated *in planta* only in response to isolate 12SD80, which makes the involvement of this ROS unlikely in the resistance of *Brachypodium* to *P. coronata* f. sp. *avenae.* In contrast to H_2O_2, phytohormones may play a thus far undefined role in modulating NHR in *Brachypodium* to rust pathogens.

Plant responses to pathogens are partly regulated through a complex interplay between salicylic acid (SA), ethylene (ET) and jasmonic acid (JA) signaling pathways (Denancé et al. 2013). Gill et al. (2015) found that several defense-related genes involved in SA, ET, and JA signaling pathways were induced in *Brachypodium* accessions infected with *P. emaculata*. In our study, upregulation of several SA-responsive genes and the key ethylene response regulator *ERF1* was detected, suggesting that SA and ET-signaling pathways may positively regulate NHR against *P. coronata* f. sp. *avenae*. The *Pathogenesis-related* (*PR*) genes *PR1* and *PR5,* which are typical markers of ETI (Kouzai et al. 2016, Sels et al. 2008) were upregulated, further supporting a role for effector recognition in this resistance. JA biosynthesis genes were not induced, making this

hormone unlikely to play an active role in this NHR response. In contrast, *ERF1*, which acts as a key regulatory element in the ET/JA-dependent defense responses, was upregulated suggesting that ET-responsive genes may enhance NHR (Berrocal-Lobo et al. 2002; Lorenzo et al. 2003; Müller and Munné-Bosch 2015). *Phenylalanine Ammonia-Lyase* (*PAL*) is a key enzyme in biosynthesis of polyphenolic compounds and lignin precursors and is often associated with host resistance responses against pathogens (Kalisz et al. 2015). Lignin deposition in response to pathogen attack is usually correlated with reinforcement of the cell wall and enhanced resistance (Miedes et al. 2014). Upregulation of *PAL* does not appear to play a significant role in the responses of *B. distachyon* to *P. coronata* f. sp. *avenae;* however, induction of *CAD* may point to cell wall alterations in response to isolates 12SD80 and 203. A genome-wide transcriptional analysis of the interaction of *P. coronata* f. sp. *avenae* with ABR6 and Bd21 will help to elucidate the involvement of some of these specific processes in NHR, including phytohormone regulation.

Extensive *P. coronata* f. sp. *avenae* growth in some *Brachypodium* accessions implies that the pathogen is capable of nutrient accession for a period of time and possibly able to target susceptibility factors conserved between *Brachypodium* and oat. Little is known about the mechanisms underlying rust susceptibility. Pathogens can alter sugar partitioning in the host to accommodate their growth (Lapin and Van den Ackerveken 2013), and thus sugar transporter proteins (STPs) may be targeted by rust fungi to increase nutrient availability (Dodds and Lagudah 2016). The wheat *STP13* hexose transporter is implicated in supporting rust pathogens as mutations in this gene leads to

511 broad-spectrum resistance (Moore et al. 2015). We examined the expression of the
512 ortholog of wheat *STP13* in *Brachypodium* during infection by *P. coronata* f. sp. *avenae*.
513 Interestingly, the highest levels of *BdSTP13* expression were obtained in accession Bd21,
514 which is subjected to more rust growth than ABR6, suggesting that the gene may indeed
515 serve as a susceptibility factor. Our results are consistent with previous findings that show
516 that expression of *Lr67,* and its homoeologs in wheat peaks at 24 hpi upon infection with
517 the leaf rust fungus, *Puccinia triticina*. Gene expression analysis of *Lr67* as well as other
518 *STP13* genes in *Arabidopsis* and grapevine, indicates that the gene is also induced in
519 response to pathogens (Hayes et al. 2010; Lemonnier et al. 2014; Moore et al. 2015).
520 These observations provide a basis to study the contribution of sugar transport to rust
521 susceptibility in an experimental system that is not as complex as in hexaploid oat and
522 wheat.
523
524 Several studies have demonstrated the value of mining wild relatives of crop species to
525 introduce disease resistance. Effective race-specific rust resistance has been
526 introgressed into wheat (*Triticum aestivum*) from related species, such as the *Sr50* gene
527 from rye (*Secale cereale*), which confers resistance to wheat stem rust by recognition of
528 the corresponding AvrSr50 effector of *P. graminis* f. sp. *tritici* (Chen et al. 2017; Mago et
529 al. 2015). Similarly, functional transfer of the pigeonpea (*Cajanus cajan*) *CcRpp1*
530 resistance gene into soybean confers resistance against soybean rust (*Phakopsora*
531 *pachyrhizi*), which demonstrates how heterologous resistance transgenes can be used
532 for crop improvement (Kawashima et al. 2016). This interspecies transfer of disease
533 resistance highlights the possibility that *Brachypodium* genes that confer NHR to *P.*

534 *coronata* f. sp. *avenae* could potentially be transferred to oat and provide disease
535 resistance. As a next step, we are utilizing an ABR6 x Bd21 mapping population to identify
536 resistance loci that could be tested in *A. sativa*. In summary, our findings indicate that
537 *Brachypodium* is a suitable species for evaluating NHR to *P. coronata* f. sp. *avenae* and
538 is a potential source of novel disease resistance for oat. The rapid expansion of genomic
539 resources, including fully sequenced genomes and assessment of genetic diversity
540 among *Brachypodium* genotypes (International *Brachypodium* Initiative 2010; Gordon et
541 al. 2014, 2017) enables this species to be exploited for engineering disease resistance in
542 closely related crop species.
543

544 **Acknowledgements**

545

546 We acknowledge support by the University of Minnesota Experimental Station USDA-
547 NIFA Hatch/Figueroa project MIN-22-058, as well as the USDA-ARS-The University of
548 Minnesota Standard Cooperative Agreement (3002-11031-00053115) between S.F.K
549 and M.F. M.J.M. is supported by the Gatsby Foundation and Biotechnology and Biological
550 Sciences Research Council (BB/P012574/1). We thank P.N. Dodds and E. Henningsen
551 for discussions and comments during manuscript preparation, as well as Roger Caspers
552 and Lief van Lierop for technical support.
553

554

555 **Literature cited**

556

557 Adlung, N., Prochaska, H., Thieme, S., Banik, A., Blüher, D., John, P., et al. 2016. Non-
558 host resistance induced by the Xanthomonas effector XopQ is widespread within the
559 genus Nicotiana and functionally depends on EDS1. Front. Plant Sci. 7.

560

561 Ayliffe, M., Singh, D., Park, R., Moscou, M.J., and Pryor, T. 2013. The infection of
562 *Brachypodium distachyon* with selected grass rust pathogens. Mol. Plant Microbe
563 Interact. 26:946-957.

564

565 Barbieri, M., Marcel, T.C., and Niks, R.E. 2011. Host status of false brome grass to the
566 leaf rust fungus *Puccinia brachypodii* and the stripe rust fungus *P. striiformis.* Plant Dis.
567 95:1339-1345.

568

569 Berrocal-Lobo, M., Molina, A., and Solano, R. 2002. Constitutive expression of
570 ETHYLENE-RESPONSE-FACTOR1 in *Arabidopsis* confers resistance to several
571 necrotrophic fungi. Plant J. 29:23-32.

572

573 Bettgenhaeuser, J., Gilbert, B., Ayliffe, M., and Moscou, M. J. 2014. Nonhost resistance
574 to rust pathogens–a continuation of continua. Front. Plant Sci. 5:664.

575

576 Bettgenhaeuser J, Corke, F.M.K., Opanowicz, M., Green, P., Hernández-Pinzón, I.,
577 Doonan, J.H., et al. 2017. Natural variation in *Brachypodium* links vernalization and

578 flowering time loci as major flowering determinants. Plant Physiol. 173:256-268.

579

580 Bossolini, E., Wicker, T., Knobel, P. A., and Keller, B. 2007. Comparison of orthologous
581 loci from small grass genomes *Brachypodium* and rice: implications for wheat genomics
582 and grass genome annotation. Plant J. 49:704-717.

583

584 Cantu, D., Segovia, V., MacLean, D., Bayles, R., Chen, X., Kamoun, S., et al. 2013.
585 Genome analyses of the wheat yellow (stripe) rust pathogen *Puccinia striiformis* f. sp.
586 *tritici* reveal polymorphic and haustorial expressed secreted proteins as candidate
587 effectors. BMC Genomics 14:270.

588

589 Carson, M.L. 2011. Virulence in oat crown rust (*Puccinia coronata* F. sp. *avenae*) in the
590 United States from 2006 through 2009. Plant Dis. 95:1528-1534.

591

592 Catanzariti, A.M., Dodds, P.N., Lawrence, G.J., Ayliffe, M.A., and Ellis, J.G. 2006.
593 Haustorially expressed secreted proteins from flax rust are highly enriched for avirulence
594 elicitors. Plant Cell 18:243-256.

595

596 Chang, T.D., and Sadmaga, K. 1964. Crosses of six rnonosomics in *Avena sativa* L. with
597 varieties, species and chlorophyll mutants. Crop Sci. 4: 589-593.

598

599 Chen, J., Upadhyaya, N.M., Ortiz, D., Sperschneider, J., Li, F., Bouton, C., et al. 2017.
600 Loss of *AvrSr50* by somatic exchange in stem rust leads to virulence for *Sr50* resistance

in wheat. Science 358:1607-1610.

Chong, J., Leonard, K.J., and Salmeron, J.J. 2000. A North American system of nomenclature for *Pucinia coronata* f.sp. *avenae*. Plant Dis. 84:580-585.

Dawson, A.M., Bettgenhaeuser, J., Gardiner, M., Green, P., Hernández-Pinzón, I., Hubbard, A., et al. 2015. The development of quick, robust, quantitative phenotypic assays for describing the host-nonhost landscape to stripe rust. Front. Plant Sci. 6:876.

Denancé, N., Sánchez-Vallet, A., Goffner, D., and Molina, A. 2013. Disease resistance or growth: the role of plant hormones in balancing immune responses and fitness costs. Front. Plant Sci. 4:155.

Dodds, P.N., and Rathjen, J.P. 2010. Plant immunity: towards an integrated view of plant-pathogen interactions. Nat. Rev. Genet. 11:539-548.

Dodds, P.N., and Lagudah, E.S. 2016. Starving the enemy. Science. 354:1377-1379.

Duplessis, S., Cuomob, C.A., Linc, Y.C., Aertsd, A., Tisseranta, E., Veneault-Fourreya, C., et al. 2011. Obligate biotrophy features unraveled by the genomic analysis of rust fungi. Proc. Natl. Acad. Sci. U.S.A. 108:9166-9171.

Ellis, J.G., Lagudah, E.S., Spielmeyer, W., and Dodds, P.N. 2014. The past, present and

624 future of breeding rust resistant wheat. Front. Plant Sci. 5:641.

625

626 Figueroa, M., Alderman, S., Garvin, D.F., and Pfender, W.F. 2013. Infection of
627 *Brachypodium distachyon* by formae speciales of *Puccinia graminis:* Early infection
628 events and host-pathogen incompatibility. PLoS One 8:e56857.

629

630 Figueroa, M., Castell-Miller, C.V., Li, F., Hulbert, S.H., and Bradeen, J.M. 2015. Pushing
631 the boundaries of resistance: insights from *Brachypodium*-rust interactions. Front. Plant
632 Sci. doi.org/10.3389/fpls.2015.00558.

633

634 Flor, H. 1971. Current status of the gene-for-gene concept. Annu. Rev. Phytopathol.
635 9:275-296.

636

637 Garnica, D.P., Nemri, A., Upadhyaya, N.M., Rathjen, J.P., and Dodds, P.N. 2014. The ins
638 and outs of rust haustoria. PLoS Pathog. 10:e1004329.

639

640 Garvin, D.F., Gu, Y.Q., Hasterok, R., Hazen, S.P., Jenkins, G., Mockler, T.C., et al.
641 2008. Development of genetic and genomic research resources for *Brachypodium*
642 *distachyon*, a new model system for grass crop research. Crop Sci. 48:S69-S84.

643

644 Garvin, D.F. 2011. Investigating rust resistance with the model grass *Brachypodium*, in
645 *Proceedings of the 2011 Borlaug Global Rust Initiative Technical Workshop,* June 13–19,
646 ed. R. McIntosh (St. Paul, MN), 89-91.

Giesbers, A.K.J., Pelgrom, A.J.E., Visser, R.G.F., Niks, R.E., Van den Ackerveken, G., and Jeuken, M.J.W. 2017. Effector-mediated discovery of a novel resistance gene against *Bremia lactucae* in a nonhost lettuce species. New Phytol. 216:915–926

Gill, U.S., Uppalapati, S.R., Nakashima, J., and Mysore, K.S. 2015. Characterization of *Brachypodium distachyon* as a nonhost model against switchgrass rust pathogen *Puccinia emaculata*. BMC Plant Biol. 15:113.

Gordon, S.P., Priest, H., Des Marais, D.L., Schackwitz, W., Figueroa, M., Martin, J., et al. 2014. Genome diversity in *Brachypodium distachyon*: Deep sequencing of highly diverse inbred lines. Plant J. 79:361-374.

Gordon, S.P., Contreras-Moreira, B., Woods, D.P., Des Marais, D.L., Burgess, D., Shu, S., et al. 2017. Extensive gene content variation in the *Brachypodium distachyon* pan-genome correlates with population structure. Nat. Commun. 8:2184.

Goritschnig, S., Krasileva, K.V., Dahlbeck, D., and Staskawicz, B.J. 2012. Computational prediction and molecular characterization of an oomycete effector and the cognate *Arabidopsis* resistance gene. PLoS Genet 8: e1002502.

Hacquard, S., Joly, D.L., Lin, Y.C., Tisserant, E., Feau, N., Delaruelle C., et al. 2012. A comprehensive analysis of genes encoding small secreted proteins identifies candidate

effectors in *Melampsora larici-populina* (Poplar Leaf Rust). Mol. Plant Microbe Interact. 25:279-293.

Hayes, M.A., Feechan, A., and Dry, I.B. 2010. Involvement of abscisic acid in the coordinated regulation of a stress-inducible hexose transporter (VvHT5) and a cell wall invertase in grapevine in response to biotrophic fungal infection. Plant Physiol. 153:211-221.

Heath, M.C. 2000. Nonhost resistance and nonspecific plant defenses. Curr. Opin. Plant Biol. 3:315-319.

Holland, J.B., and Munkvold, G.P. 2001. Genetic relationships of crown rust resistance, grain yield, test weight, and seed weight in oat. Crop Sci. 41:1041-1050.

Hong, S.Y., Seo, P.J., Yang, M.S., Xiang, F., and Park, C.M. 2008. Exploring valid reference genes for gene expression studies in *Brachypodium distachyon* by real-time PCR. BMC plant biol. 8:112.

Kalisz, S., Oszmiański, J., and Wojdylo, A., 2015. Increased content of phenolic compounds in pear leaves after infection by the pear rust pathogen. Physiol. Mol. Plant Pathol. 91:113-119.

693 Kawashima, C.G., Guimaraes, G.A., Nogueira, S.R., MacLean, D., Cook, D.R.,
694 Steuernagel, B., et al. 2016. A pigeonpea gene confers resistance to Asian soybean rust
695 in soybean. Nat. Biotechnol. 34:661-665.
696
697 Kouzai, Y., Kimura, M., Yamanaka, Y., Watanabe, M., Matsui, H., and Yamamoto, M.
698 2016. Expression profiling of marker genes responsive to the defense-associated
699 phytohormones salicylic acid, jasmonic acid and ethylene in *Brachypodium distachyon*.
700 BMC Plant Biol. 16:59.
701
702 Lapin, D., and Van den Ackerveken, G. 2013. Susceptibility to plant disease: More than
703 a failure of host immunity. Trends Plant Sci. 18:546-554.
704
705 Lee, H. A., Kim, S. Y., Oh, S. K., Yeom, S. I., Kim, S. B., Kim, M. S., et al. 2014. Multiple
706 recognition of RXLR effectors is associated with nonhost resistance of pepper against
707 *Phytophthora infestans*. New Phytol. 203:926-938.
708
709 Lemonnier, P., Gaillard, C., Veillet, F., Verbeke, J., Lemoine, R., Coutos-Thévenot, P.,
710 et al. 2014. Expression of Arabidopsis sugar transport protein STP13 differentially affects
711 glucose transport activity and basal resistance to *Botrytis cinerea*. Plant Mol. Biol. 85:473-
712 484.
713
714 Livak, K.J., and Schmittgen, T.D. 2001. Analysis of relative gene expression data using
715 real-time quantitative PCR and the 2(-Delta Delta C(T)). Methods. 25:402-408.

716

717 Lopez-Alvarez, D., Lopez-Herranz, M.L., Betekhtin, A., and Catalan, P. 2012. A DNA
718 barcoding method to discriminate between the model plant *Brachypodium distachyon* and
719 its close relatives *B. stacei* and *B. hybridum* (Poaceae). PLoS One 7:e51058.

720

721 Lorenzo, O., Piqueras, R., Sánchez-Serrano, J.J., and Solano, R. 2003. ETHYLENE
722 RESPONSE FACTOR1 Integrates Signals from Ethylene and Jasmonate Pathways in
723 Plant Defense. Plant Cell. 15:165-178.

724

725 Mago, R., Zhang, P., Vautrin, S., Šimková, H., Bansal, U., Luo, M. C., et al. 2015. The
726 wheat Sr50 gene reveals rich diversity at a cereal disease resistance locus. Nat. Plants.
727 1:15186.

728

729 Maia, T., Badel, J.L., Marin-Ramirez, G., Rocha, C.M., Fernandes, M.B., da Silva, J.C.F.,
730 et al. 2017. The *Hemileia vastatrix* effector HvEC-016 suppresses bacterial blight
731 symptoms in coffee genotypes with the SH1 rust resistance gene. New Phytol. 213:1315-
732 1329.

733

734 Mandadi, K.K. and Scholthof, K.B.G. 2012. Characterization of a viral synergism in the
735 monocot *Brachypodium distachyon* reveals distinctly altered host molecular processes
736 associated with disease. Plant Physiol. 160:1432-1452.

737

738 Miedes, E., Vanholme, R., Boerjan, W., and Molina, A. 2014. The role of the secondary

739 cell wall in plant resistance to pathogens. Front. Plant Sci. 5:358.

740

741 Miller, M. E., Zhang, Y., Omidvar, V., Sperschneider, J., Schwessinger, B., Raley, C., et
742 al. 2018. *De novo* assembly and phasing of dikaryotic genomes from two isolates of
743 *Puccinia coronata* f. sp. *avenae*, the causal agent of oat crown rust. mBio 9:e01650-17.

744

745 Moore, J.W., Herrera-Foessel, S., Lan, C., Schnippenkoetter, W., Ayliffe, M., Huerta-
746 Espino, J., et al. 2015. A recently evolved hexose transporter variant confers resistance
747 to multiple pathogens in wheat. Nat. Genet. 47:1494-1498.

748

749 Müller, M., and Munné-Bosch, S. 2015. Ethylene response factors: A key regulatory hub
750 in hormone and stress signaling. Plant Physiol. 169:32-41.

751

752 Mur, L.A., Allainguillaume, J., Catalan, P., Hasterok, R., Jenkins, G., Lesniewska, K.,
753 Thomas, L., and Vogel, J. 2011. Exploiting the *Brachypodium* tool box in cereal and grass
754 research. New Phytol. 191:334–347.

755

756 Mysore, K.S., and Ryu, C.M. 2004. Nonhost resistance: How much do we know? Trends
757 Plant Sci. 9:97-104.

758

759 Nazareno, E.S., Li, F., Smith, M., Park, R.F., Kianian, S.F., and Figueroa, M. 2017.
760 *Puccinia coronata* f. sp. *avenae*: a threat to global oat production. Mol. Plant Pathol. DOI:
761 10.1111/mpp.12608.

Nemri, A., Saunders, D.G.O., Anderson, C., Upadhyaya, N.M., Win, J., Lawrence, G.J., et al. 2014. The genome sequence and effector complement of the flax rust pathogen *Melampsora lini*. Front. Plant Sci. 5:98.

Nurnberger, T., and Lipka, V. 2005. Non-host resistance in plants: new insights into an old phenomenon. Mol. Plant Pathol. 6:335-345.

Panstruga, R., and Dodds, P.N. 2009. Terrific protein traffic: the mystery of effector protein delivery by filamentous plant pathogens. Science. 324:748-750.

Periyannan, S., Moore, J., Ayliffe, M., Bansal, U., Wang, X., Huang, L., et al. 2013. The gene *Sr33*, an ortholog of barley *Mla* genes, encodes resistance to wheat stem rust race Ug99. Science. 341:786-788.

Periyannan, S., Milne, R.J., Figueroa, M., Lagudah, E.S. and Dodds, P.N. 2017. An overview of genetic rust resistance: from broad to specific mechanisms. PLoS Pathog. 13: e1006380.

Ravensdale, M., Nemri, A., Thrall, P.H., Ellis J.G., and Dodds, P.N. 2011. Co-evolutionary interactions between host resistance and pathogen effector genes in flax rust disease. Mol. Plant Pathol. 12:93-102.

785 Rutter, W.B., Salcedo, A., Akhunova, A., He, F., Wang, S., Liang, H., et al. 2017.
786 Divergent and convergent modes of interaction between wheat and *Puccinia graminis* f.
787 sp. *tritici* isolates revealed by the comparative gene co-expression network and genome
788 analyses. BMC Genomics. 18:291.
789
790 Salcedo, A., Rutter, W., Wang, S., Akhunova, A., Bolus, S., Chao, S., et al. 2017.
791 Variation in the *AvrSr35* gene determines *Sr35* resistance against wheat stem rust race
792 Ug99. Science. 358:1604-1606.
793
794 Schulze-Lefert, P., and Panstruga, R. 2011. A molecular evolutionary concept connecting
795 nonhost resistance, pathogen host range, and pathogen speciation. Trends Plant Sci. 16:
796 117-125.
797
798 Sels, J., Mathys, J., De Coninck, B.M.A., Cammue, B.P.A., and De Bolle, M.F.C. 2008.
799 Plant pathogenesis-related (PR) proteins: A focus on PR peptides. Plant Physiol. Bioch.
800 46:941-950.
801
802 Simons, M.D. 1985. Crown rust. In: Roelfs AP, Bushnell WR (eds) The cereal rusts, vol.
803 II, disease, distribution, epidemiology and control. Academic, New York, USA, pp 131-
804 172.
805
806 Stassen, J. H. M., den Boer, E., Vergeer, P. W. J., Andel, A., Ellendorff, U., Pelgrom, K.,
807 et al. 2013. Specific in planta recognition of two GKLR proteins of the downy mildew

Bremia lactucae revealed in a large effector screen in lettuce. Mol. Plant. Microbe. Interact. 26:1259-70.

Sumit, R., Sahu, B. B., Xu, M., Sandhu, D., and Bhattacharyya, M. K. 2012. Arabidopsis nonhost resistance gene PSS1 confers immunity against an oomycete and a fungal pathogen but not a bacterial pathogen that cause diseases in soybean. BMC Plant Biol. 12:1.

The International *Brachypodium* Initiative. 2010. Genome sequencing and analysis of the model grass *Brachypodium distachyon*. Nature. 463:763-768.

Thordal-Christensen, H., Zhang, Z., Wei, Y., and Collinge, D.B. 1997. Subcellular localization of H_2O_2 in plants. H_2O_2 accumulation in papillae and hypersensitive response during the barley-powdery mildew interaction. Plant J. 11:1187-1194.

Thordal-Christensen, H. 2003. Fresh insights into processes of nonhost resistance. Curr. Opin. Plant Biol. 6:351-357.

Toruno, T.Y., Stergiopoulos, I., and Coaker, G. 2016. Plant-pathogen effectors: Cellular probes interfering with plant defenses in spatial and temporal manners. Annu. Rev. Phytopathol. 54:419-441.

831 Vogel, J.P., Tuna, M., Budak, H., Huo, N., Gu, Y.Q., and Steinwand, M.A. 2009.
832 Development of SSR markers and analysis of diversity in Turkish populations of
833 *Brachypodium distachyon*. BMC Plant Biol. 9:88.

834

835 Zipfel, C. 2008. Pattern-recognition receptors in plant innate immunity. Curr. Opin.
836 Immunol. 20:10-16.

837

Table 1. Variation of symptoms in *Brachypodium* accessions infected with *P. coronata* f. sp. *avenae* isolates.

	12SD80		203		12NC29	
Accessions	**Chlorosis**	**Necrosis**	**Chlorosis**	**Necrosis**	**Chlorosis**	**Necrosis**
ABR6	-	+	-	-	-	+
ABR7	+	+	+	+	+	+
Adi12	+++	+	++	+	+	+
Adi13	+++	++	+	+++	++++	++
Adi15	++	++	+++	+	+++	++
Bd1-1	+++	++++	+++	+	+	++
Bd18-1	-	+	+	+	+++	++
Bd21	++	+++	+++	+++	++	++
Bd21-3	++	+++	+++	++	++++	+++
Bd2-3	+++	+++	+	++	+	+
Bd29-1	++	++++	+	+	+	+++
Bd30-1	+	++	+	+	+	+++
Bd3-1	++	++++	+	+++	+++	++
BdTR10H	++	++	+	+	++	++
BdTR13K	+	++	+	++	+	++
Foz1	+	+	+++	++++	+	-
J6.2	+	+	+	+	+	+
Jer1	+	+++	-	+	+	++
Koz5	++	++	+++	++	+++	++
Luc1	+	+	+	-	++	+
Mon3	++	++++	+	+	+++	+
Tek4	-	+++	+	-	+	+
***Bel1**	+	++	+	+	+	++++
***Bou1**	+	+	+	++	-	+++
***Pob1**	-	+++	+	+	+	+

Accessions with asterisks correspond to *B. hybridum* and those without asterisk are *B. distachyon* accessions. Symbols “+” and “-” show presence or absence of macroscopic symptoms, respectively, and number of “+” indicates symptom severity with ++++ as maximum level.

Table 2. Histological analysis of H_2O_2 accumulation in *B. distachyon* accessions ABR6 and Bd21 in response to *P. coronata* f. sp. *avenae* infection.

	1 dpi		2 dpi		3 dpi		4 dpi		5 dpi	
	ABR6	**Bd21**	**ABR6**	**Bd21**	**ABR6**	**Bd21**	**ABR6**	**Bd21**	**ABR6**	**Bd21**
12SD80	-	-	+ (8)	-	+ (9)	-	+ (14)	+ (6)	+ (16)	+ (12)
203	-	-	-	-	-	-	-	-	-	-
12NC29	-	-	-	-	-	-	-	-	-	-

Presence (+) or absence (-) of H_2O_2 accumulation is indicated per number of days post inoculation (dpi). Numbers in parentheses indicate the sum of sites displaying H_2O_2 accumulation in three biological replicates. Each biological replicate consisted of 100 infection sites.

Figure legends

Fig. 1. Infection of oat and *Brachypodium* accessions with *P. coronata* f. sp*. avenae.* **A**. Virulence phenotypes of *P. coronata* f. sp*. avenae* isolates on oat differentials with infection types of “0”, “0;”, “;”, “;C”, “1;”, “1”, “2”, “3”, “3+”, and “4” converted to a 0-9 numeric scale, respectively, for heat map generation. **B, C**. Formation of pustules and sporulation on infected susceptible oat leaves (Marvelous), respectively. **D, E**. Variation of infection symptoms and fungal colonization, respectively, on four *Brachypodium* accessions. **F**. Absence (-) or presence (+) of chlorosis and/or necrosis in *Brachypodium* accessions inoculated with *P. coronata* f. sp*. avenae* at 14 dpi. Level of symptom severity is indicated by the number of “+” characters. Symptoms correspond to the representative isolate 12SD80, except for the absence of necrosis which corresponds to isolate 203. Scale bars indicate 2 mm (B, D, F), 0.5 mm (C, top), 0.25 mm (C, bottom) and 0.5 mm (E)

Fig. 2. Colonization of *Brachypodium* accessions by *P. coronata* f. sp*. avenae*. **A**. Fungal growth estimates in foliar tissue for isolates 12SD80, 203, and 12NC29 depicted by the percentage of colonized area at 14 dpi. Crown rust susceptible oat (*A. sativa*) variety Marvelous serves as positive experimental control. Each bar represents a mean value in one biological replicate and error bars represent standard error of mean of three technical replicates. **B**. Quantification of fungal biomass for each rust isolate in *B. distachyon* accessions ABR6 (blue line) and Bd21 (orange line). Error bars represent standard error of mean of at least four biological replicates.

894

895 **Fig. 3.** Fungal development of *P. coronata* f. sp*. avenae* in *Brachypodium* accessions. **A.**
896 Illustration of *P. coronata* f. sp*. avenae* development in the plant. Germinated
897 urediniospores (GS) form a penetration structure appressorium (AP) over a stoma. The
898 fungus enters the mesophyll cavity and differentiates a substomatal vesicle (SV) and
899 infection hypha. The establishment of a rust colony (EC) begins with the formation of a
900 feeding structure (haustorium) which requires differentiation of a haustorial mother cell
901 (HMC) near the hyphal tip. To undergo HMC formation, the rust fungus must come in
902 contact with a mesophyll cell. **B.** Bars show the percentage of interaction sites with
903 germinated urediniospores (GS, light blue), formation of appressorium (AP, orange),
904 substomatal vesicle (SV, gray), haustorium-mother cell (HMC, yellow), established colony
905 (EC, dark blue), and EC with sporulation (SP, green) in a sample of 100 infection sites
906 per biological replicate. Error bars represent standard error of mean of three biological
907 replicates.

908

909 **Fig. 4.** Expression profiling of various defense-related genes in *Brachypodium* accessions
910 in response to *P. coronata* f. sp*. avenae*. Gene expression (fold-change) relative to mock
911 inoculations in rust infected ABR6 (blue) and Bd21 (orange) plants of *Aberrant Growth*
912 *Defects* 2 (*AGD2*), *Alternative Oxidase* (*AOX1A*), *Pathogenesis-related* (*PR*) *genes,*
913 *Ethylene Response Factor* 1 (*ERF1*), *Phenylalanine Ammonia-Lyase* (*PAL*), and
914 *Cinnamyl Alcohol Dehydrogenase* (*CAD*). Barplots represent mean values of fold change
915 per time point. Solid colored bars indicate a fold change value of ≥ 2 whereas hatched
916 bars indicate values below this threshold. Error bars represent standard errors of three

biological replicates. Asterisks indicate statistically significant differences ($p \leq 0.05$) between ABR6 and Bd21 accessions as determined by a *t*-test.

Fig. 5. Expression profiling of *BdSTP13* in *Brachypodium* accessions in response to *P. coronata* f. sp. *avenae*. Gene expression (fold-change) relative to mock inoculations in rust infected ABR6 (blue) and Bd21 (orange) plants of the putative hexose transporter *BdSTP13.* Solid colored bars indicate a fold change value of ≥ 2 whereas hatched bars indicate values below this threshold. Error bars represent standard errors of three biological replicates. Asterisks indicate statistical significant differences ($p \leq 0.05$) between ABR6 and Bd21 accessions as determined by a t-test.

Supplementary files

Supplementary Fig. 1 shows colonization of *Brachypodium* accessions by *P. coronata* f. sp. *avenae*. Fungal growth estimate per isolate, with individual isolates 12SD80, 203 and 12NC29 shown as a percentage value relative to the accession displaying the highest level of colonization for each isolate.

Supplementary Fig. 2 shows expression profiling of various defense-related genes in *B. distachyon* accessions in response to *P. coronata* f. sp. *avenae*. Gene expression (fold-change) relative to mock inoculations in rust infected ABR6 (blue) and Bd21 (orange) plants of *Aminocyclopropane-1-carboxylic Acid Oxidase* (*ACO1*), *Lipoxygenase 2* (*LOX2*), *12-oxophytodienoate Reductase 3* (*OPR3*), *WRKY18* transcription factor, and

940 *callose synthase*. Barplots represent mean values of fold change per time point. Solid
941 colored bars indicate a fold change value of ≥ 2 whereas hatched bars indicate values
942 below this threshold. Error bars represent standard errors of three biological replicates.
943 Asterisks indicate statistical significant differences ($p \leq 0.05$) between ABR6 and Bd21
944 accessions as determined by a *t*-test.
945
946
947
948
949
950
951
952
953
954
955
956
957
958
959
960
961

Fig. 1. Infection of oat and *Brachypodium* accessions with *P. coronata* f. sp. *avenae.*

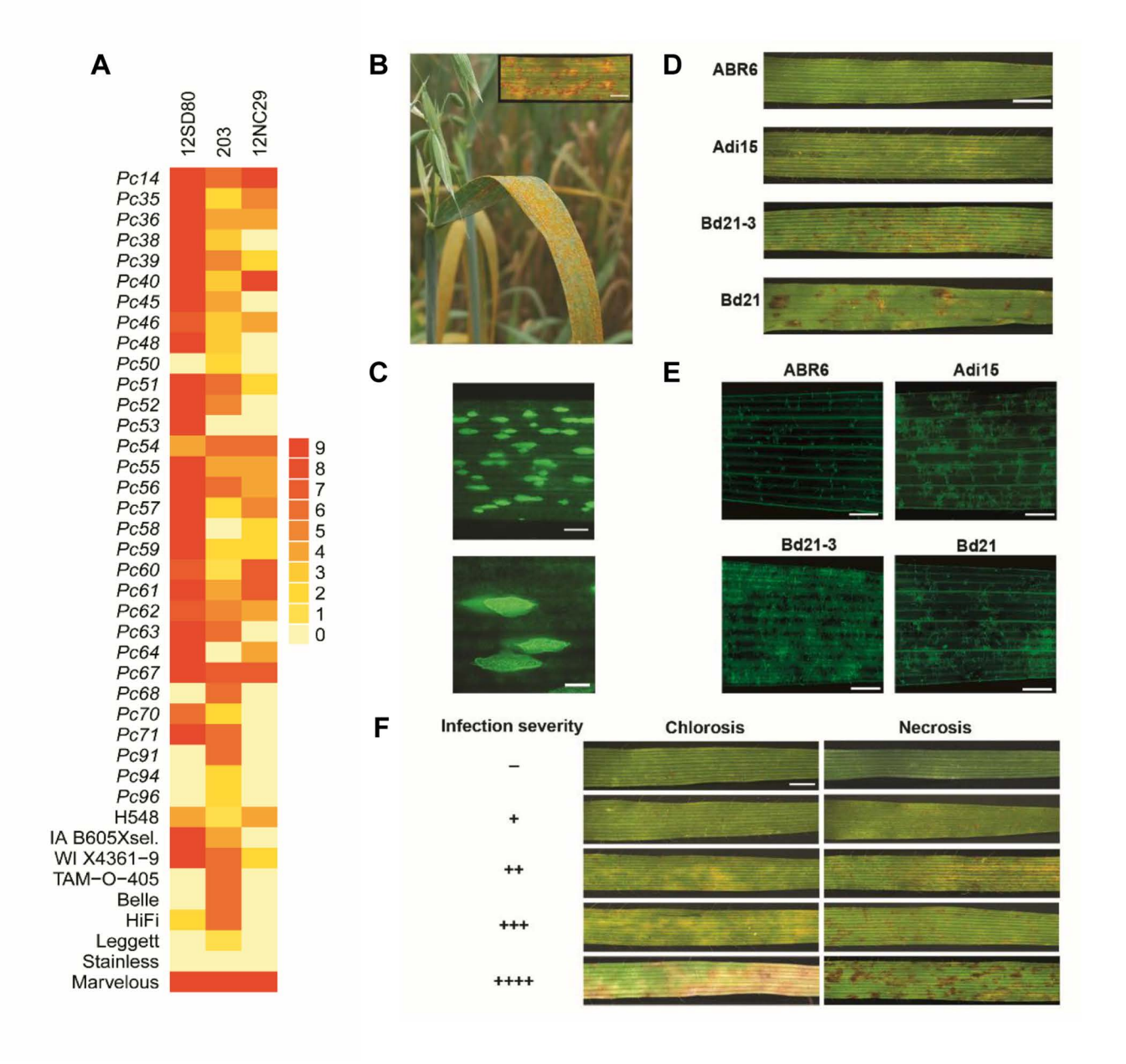
A
12SD80
203
12NC29
Pc14
Pc35
Pc36
Pc38
Pc39
Pc40
Pc45
Pc46
Pc48
Pc50
Pc51
Pc52
Pc53
Pc54
Pc55
Pc56
Pc57
Pc58
Pc59
Pc60
Pc61
Pc62
Pc63
Pc64
Pc67
Pc68
Pc70
Pc71
Pc91
Pc94
Pc96
H548
IA B605Xsel.
WI X4361-9
TAM-O-405
Belle
HiFi
Leggett
Stainless
Marvelous
9
8
7
6
5
4
3
2
1
0
B
C
D
ABR6
Adi15
Bd21-3
Bd21
E
ABR6
Adi15
Bd21-3
Bd21
F
Infection severity
Chlorosis
Necrosis
–
+
++
+++
++++

Fig. 2. Colonization of *Brachypodium* accessions by *P. coronata* f. sp. *avenae*.

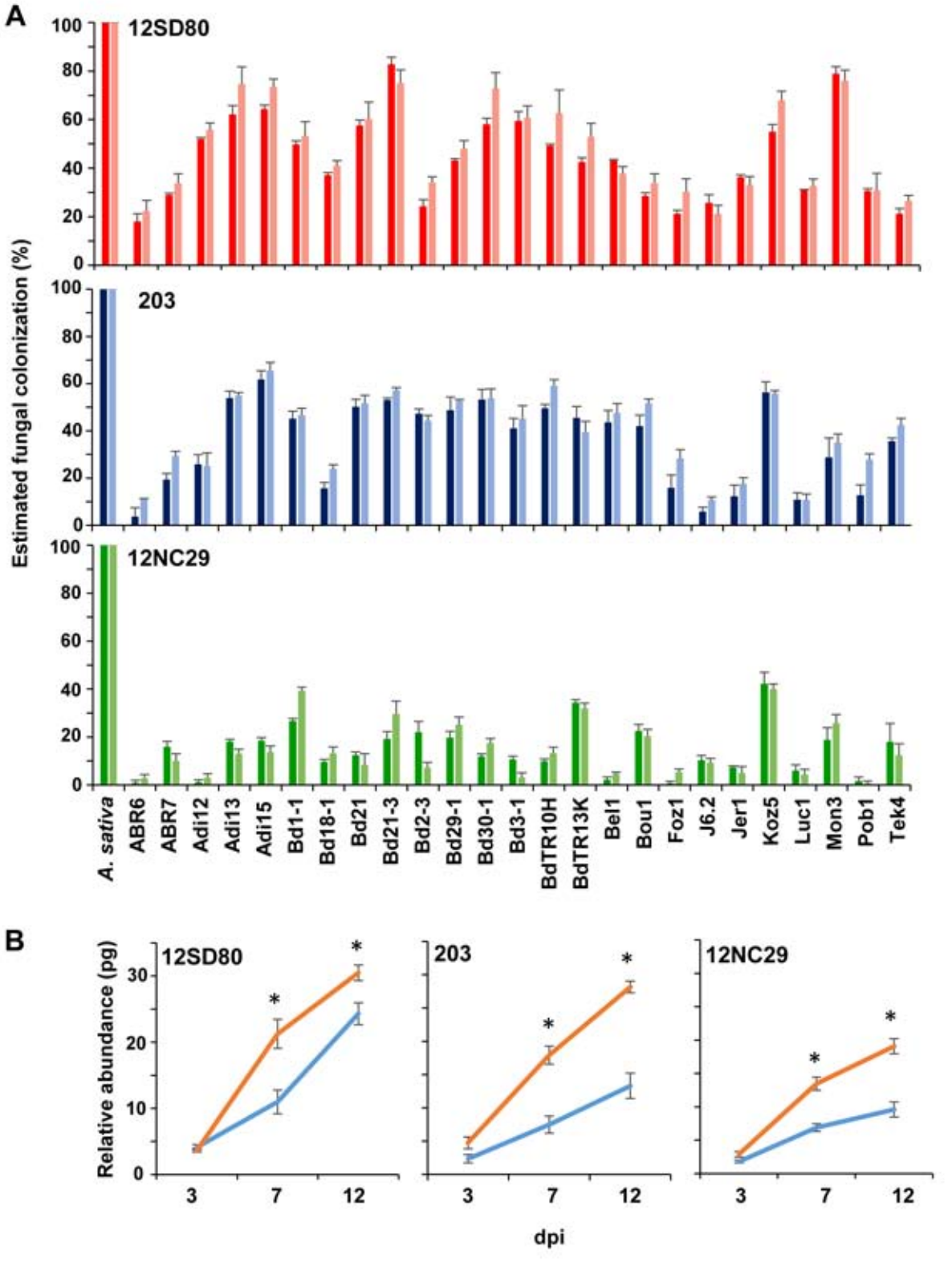
A
12SD80
203
12NC29
Estimated fungal colonization (%)
0
20
40
60
80
100
A. sativa
ABR6
ABR7
Adi12
Adi13
Adi15
Bd1-1
Bd18-1
Bd21
Bd21-3
Bd2-3
Bd29-1
Bd30-1
Bd3-1
BdTR10H
BdTR13K
Bel1
Bou1
Foz1
J6.2
Jer1
Koz5
Luc1
Mon3
Pob1
Tek4
B
12SD80
203
12NC29
Relative abundance (pg)
0
10
20
30
3
7
12
dpi
*

Fig. 3. Fungal development of *P. coronata* f. sp. *avenae* in *Brachypodium* accessions.

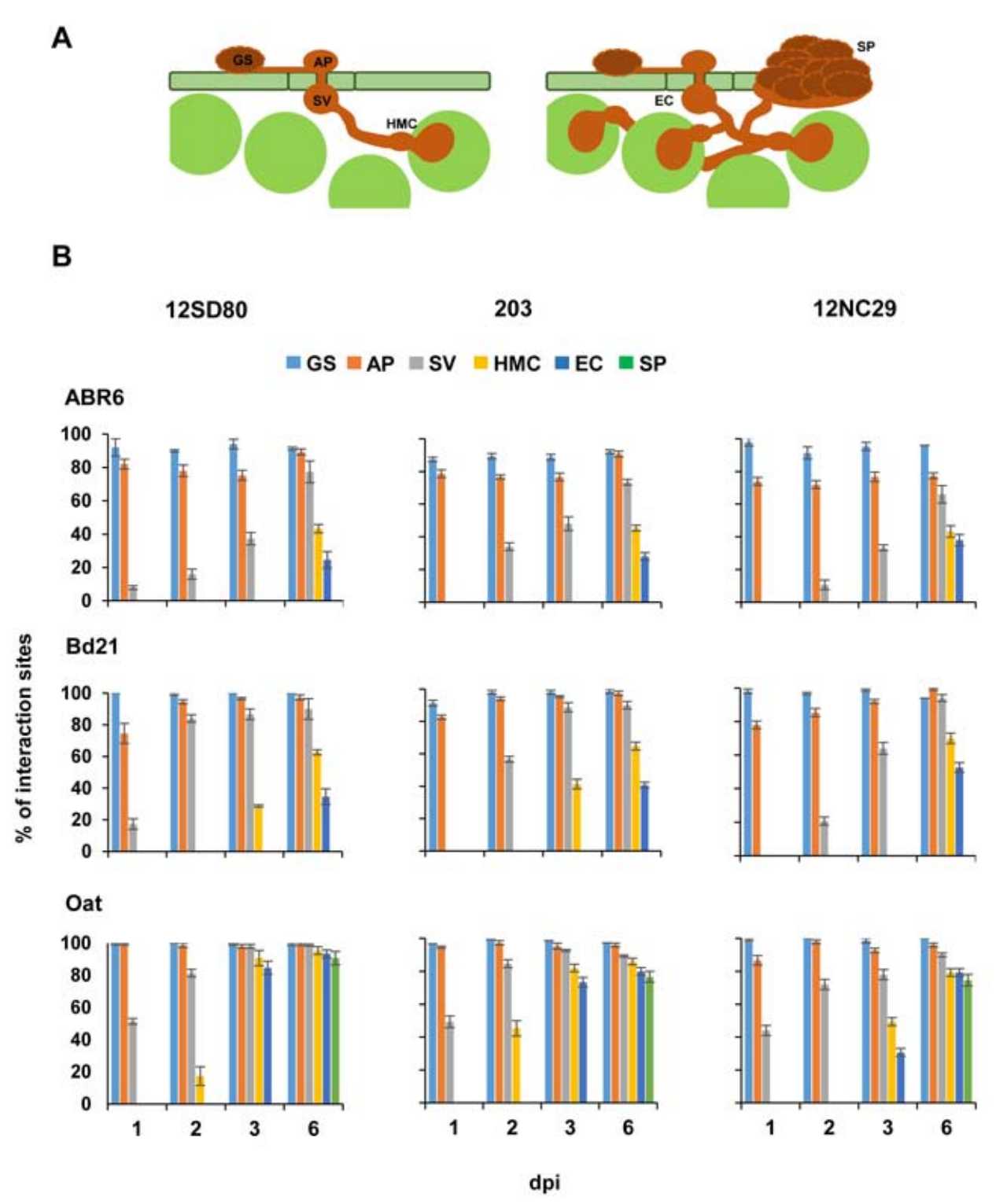
A
GS
AP
SV
HMC
EC
SP
B
12SD80
203
12NC29
GS AP SV HMC EC SP
ABR6
Bd21
Oat
% of interaction sites
100
80
60
40
20
0
1
2
3
6
dpi

Fig. 4. Expression profiling of various defense-related genes in *Brachypodium* accessions in response to *P. coronata* f. sp*. avenae*.

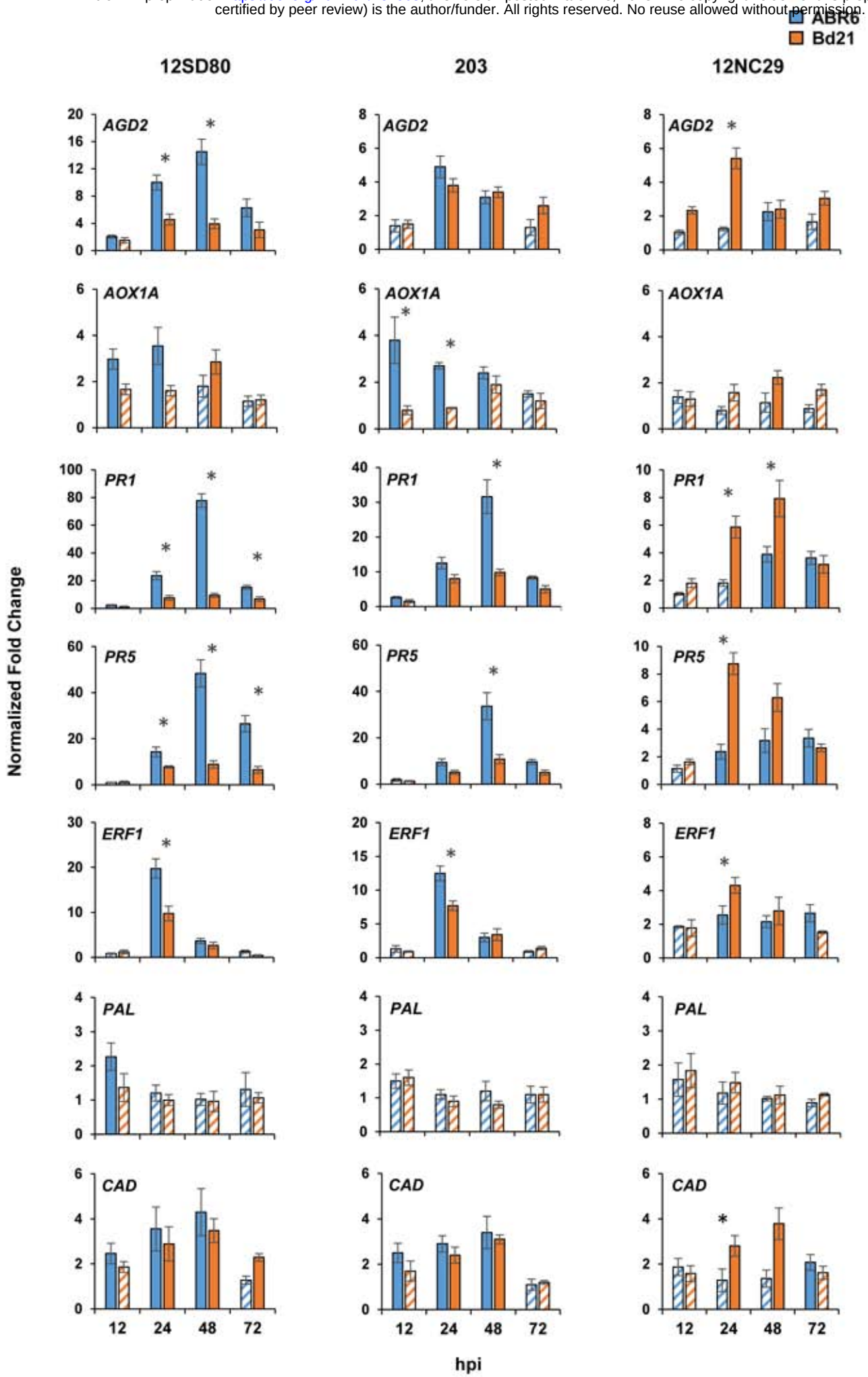

Fig. 5. Expression profiling of *BdSTP13* in *Brachypodium* accessions in response to *P. coronata* f. sp*. avenae*.

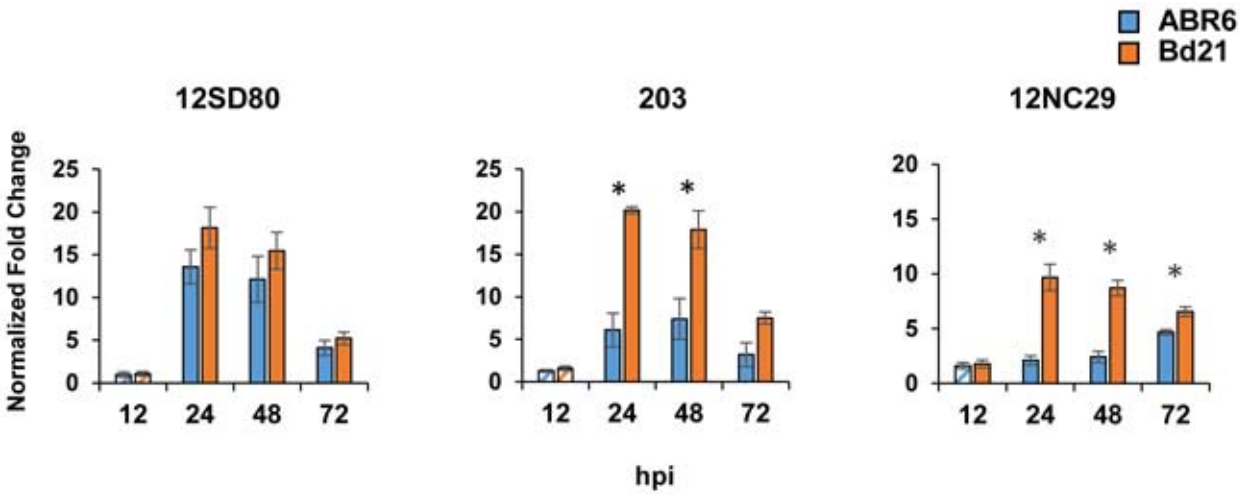
ABR6
Bd21
12SD80
203
12NC29
Normalized Fold Change
25
20
15
10
5
0
12
24
48
72
*
hpi